

# A THz-DRIVEN SPLIT RING RESONATOR FOR TEMPORAL CHARACTERIZATION OF FEMTOSECOND MeV ELECTRON BEAM\*

Y. Song<sup>†</sup>, K. Fan, Huazhong University of Science and Technology, Wuhan, China

## Abstract

The use of THz-driven split ring resonator (SRR) as a streak camera for sub-ps bunch length measurement has been proposed for a few years. Since then, the feasibility of such a method has been experimentally demonstrated for both keV and MeV electron beam. The structural dimensions of SRR has a substantial impact on the resonance frequency, the field enhancement factor and the interaction region of the streaking field, eventually determining the temporal resolution of the bunch length measurement. Here we discuss the quantitative dependence of the streaking field on the structural dimensions of SRR. Combining with an analytical streaking model, we propose a method to optimize the structural dimensions of SRR such that the finest temporal resolution is achieved with given THz pulse.

## INTRODUCTION

In the past decade, the femtosecond-level electron beam and its applications have become one of the main interests in the accelerator field. Such an electron beam is essential in many applications, such as ultrafast electron diffraction (UED) [1,2], self-amplified spontaneous emission free-electron laser (FEL) [3] and laser-plasma wakefield accelerators [4].

By using few MeV electron beam and RF compressor, electron bunch with sub-10 fs duration has been achieved [5], which pushes the requirement for the resolution of temporal characterization towards a single fs level. To data, such temporal resolution can be realized via RF deflector [5, 6]. However, the timing jitter between the RF source and laser system is at a few tens fs level which mean the uncertainty between the streak field and arrival time of the electron beam is about few tens fs. This limits the accuracy for time-of-arrival (TOA) characterization, which is very important for experiments like UED.

To provide a sub-10 fs temporal resolution for bunch length measurement and TOA characterization accuracy, a streak camera based on THz-driven split-ring resonator (SRR) is proposed a few years ago [7].

SRR is a sub-wavelength structure that focuses the incident THz radiation into the gap region, and the enhanced streaking field thus emerges in the gap. The streaking field provided by SRR is potentially up to GV/m level [8] and the frequency is about two orders higher than the RF deflector. Moreover, since the THz radiation is originated from the laser system, the streaking field is tightly synchronized to the laser system. Successful temporal characterization experiments have been demonstrated for both keV

[9] and MeV [10-12] electron beam. The experiment results indicate that SRR can provide sub-10 fs temporal resolution for bunch length measurement and sub-fs accuracy for TOA determination.

In this paper, we discuss the optimization of the geometric dimension of a square SRR. The goal of optimization is to obtain the highest streak velocity, and thus the finest temporal resolution. We first present the definition of the temporal resolution and its dependence on the parameters of SRR. Then, we use CST Microwave Studio to calculate the relevant parameters to determine the temporal resolution and therefore perform the optimization.

## TEMPORAL RESOLUTION

We first define the passing time  $T_p = h/\beta c$  where  $h$  is the length of the SRR gap in z-direction (see Fig. 1).  $\beta$  is the normalized velocity, which is about 1 for a few MeV electron beam.  $\Delta T$  denotes the full-width bunch length of electron beam. The period of the streaking field is defined as  $T$ . The resonance frequency of SRR is generally below 1 THz and the electron bunch length we measure is in the fs-level. We can assume that  $\Delta T \ll T$ .

Consider an electron with longitudinal position  $\zeta$  where  $\zeta=0$  corresponds to the bunch center and  $\zeta=\pm\Delta T/2$  the bunch head and tail. The transverse kick of such electron after passing through the SRR gap is

$$\begin{aligned} \Delta P_y(\zeta) &= -e \int_{\zeta-T_p/2}^{\zeta+T_p/2} \bar{E}_y \sin(\omega t + \varphi_0) dt \\ &= \frac{-2e\bar{E}_y}{\omega} \sin\left(\frac{\omega}{2} T_p\right) \sin(\omega\zeta + \varphi_0) \\ &\approx -2e\bar{E}_y \sin\left(\frac{\omega}{2} T_p\right) \left[ \frac{1}{\omega} \sin\varphi_0 - \cos\varphi_0 \zeta \right], \end{aligned} \quad (1)$$

where  $\varphi_0$  is the phase between the electron beam and the streaking field and  $\omega = 2\pi f_0$  is the angular resonance frequency. Note that we use the assumption  $\Delta T \ll T$ .  $\bar{E}_y$  is the equivalent streak field whose expression is

$$\bar{E}_y = \frac{\omega}{2} \frac{\int_{-\infty}^{+\infty} A(\beta ct) \cos(\omega t) dt}{\sin(\omega T_p / 2)} E_{\max}, \quad (2)$$

where  $A(\beta ct)$  is the normalized profile of the on-axis streaking field (see Fig. 2 for an example) and  $E_{\max}$  is the amplitude of the peak streaking field.

The trajectory angle of an electron after the SRR is  $\Delta P_y/P$  and thus we define the streaking velocity  $\omega_s$  is

$$\omega_s = \frac{|\Delta P_y(\Delta T/2) - \Delta P_y(-\Delta T/2)|}{P\Delta T} = \frac{2e\bar{E}_y}{P} \sin\left(\frac{\omega}{2} T_p\right).$$

Therefore, the temporal resolution of the SRR is

$$\tau_s = \frac{\sigma_{y'0}}{\omega_s} = \frac{\sigma_{y'0} P}{2e\bar{E}_y \sin(\omega T_p / 2)}, \quad (3)$$

\* Work supported by the National Natural Science Foundation of China (NSFC) 11728508

<sup>†</sup> kjfan@hust.edu.cn

where  $\sigma_{y,0}$  is the unstreaked rms divergence. Combining Eq. (2) and Eq. (3), we have

$$\tau_s \propto \frac{1}{\omega E_{\max} \int_{-\infty}^{\infty} A(\beta ct) \cos(\omega t) dt} \quad (4)$$

Equation (4) indicates that the temporal resolution of SRR is determined by the resonance frequency  $f_0$ , the peak streaking field  $E_{\max}$  and the length of the interaction region. For a given material, the resonance frequency is the function of the dimensions of SRR. The peak streaking field can be expressed as  $E_{\max} = C_{\text{enh}} E_{\text{THz}}$  where  $E_{\text{THz}}$  is the driving field strength and  $C_{\text{enh}}$  is the field enhancement factor (see Fig. 3). For a given laser system, the upper limit for  $E_{\text{THz}}$  is fixed while the dimensions of SRR determine the field enhancement factor. Note the integral term in Eq. (4) has a unit of time. The physical meaning of this term is the equivalent interaction time of the streaking process which will be referred as  $T_e$  (see Eq. (5)).

$$T_e = \int_{-\infty}^{\infty} A(\beta ct) \cos(2\pi f_0 t) dt \quad (5)$$

We denote a parameter  $F$  as a product of the resonance frequency, the field enhancement factor and the equivalent interaction time, as shown in Eq. (6). The parameter  $F$  can be regarded as an alternative measure for  $\omega_s$  and the temporal resolution.  $F$  has a unit of 1, which means it can be used as an absolute measure for the streaking performance.

$$F = f_0 C_{\text{enh}} T_e \quad (6)$$

## STRUCTURAL OPTIMIZATION

### Square SRR Model

The square SRR model we use for structural optimization is shown in Fig. 1. Here we use four dimensions ( $l$ ,  $h$ ,  $g$ ,  $w$ ) to describe a square SRR. The material of this SRR is copper.

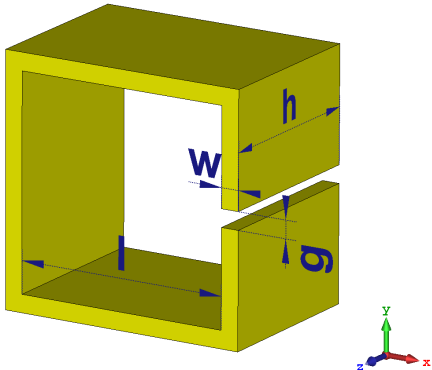


Figure 1: The dimensions of a square SRR.

The parameter  $l$  has the most impact on the resonance frequency that scales inversely with  $l$ . Moreover, the field enhancement factor is positively correlated to the ratio  $l/g$ , which increases with  $l$ . The parameter  $h$  determines the interaction region of SRR, and thus,  $A(z)$ . Figure 2 shows the field profile  $A(z)$  of an SRR with  $h=100 \mu\text{m}$  for example.

The parameter  $g$  and  $w$  also affect the streaking performance of SRR. A smaller  $g$  and  $w$  will increase the field

enhancement factor significantly. However, there is a practical consideration for the acceptance of an electron beam. In this work, we set  $g=w=10 \mu\text{m}$  to allow fC level bunch charge to pass.

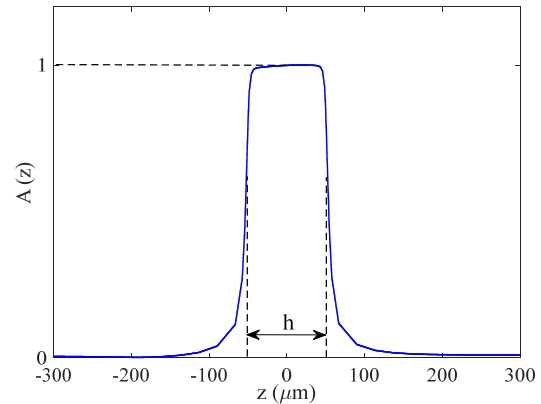


Figure 2: The normalized profile of the streaking field. The dimensions of the square profile of the SRR for are  $l=100 \mu\text{m}$ ,  $h=100 \mu\text{m}$ ,  $g=10 \mu\text{m}$  and  $w=10 \mu\text{m}$ .

To obtain the field enhancement factor  $C_{\text{enh}}$ , the THz driving field is set to 1 V/m. As we can see from Fig. 3, the field enhancement factor of this SRR is 12.455. Note that the magnetic field in the gap region is negligible compared to the electric field. Therefore, the contribution of the magnetic field will be neglected in this work.

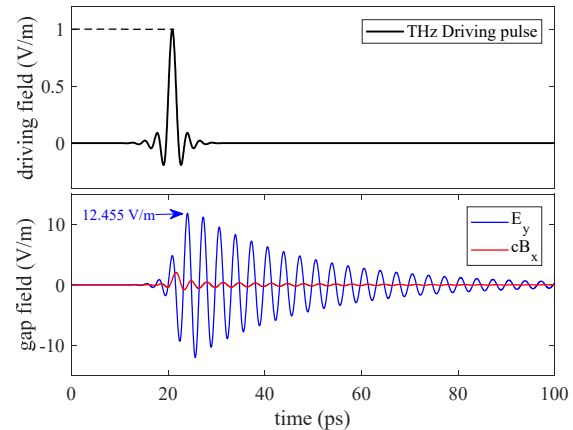


Figure 3: The THz driving field and induced gap field as functions of time. The dimensions for this SRR model are  $l=100 \mu\text{m}$ ,  $h=100 \mu\text{m}$ ,  $g=10 \mu\text{m}$  and  $w=10 \mu\text{m}$ .

### Simulation Results

We first scan the parameter  $l$  while other dimensions are fixed at  $h=100 \mu\text{m}$ ,  $g=10 \mu\text{m}$  and  $w=10 \mu\text{m}$ . Figure 4 shows the quantitative dependence of resonance frequency on  $l$ . The resonance frequency drops as we enlarge the SRR. The dependence of the field enhancement factor on  $l$  is more complicated as can be seen from Fig. 5. The streak field in the gap region has both the oscillating behavior and decaying behavior (see Fig. 3). Figure 5 shows that the field enhancement factor increases with  $l$  in general. However, due to the combination of the oscillating and decaying behavior, the dependence of field enhancement factor on  $l$  is not a smooth curve.

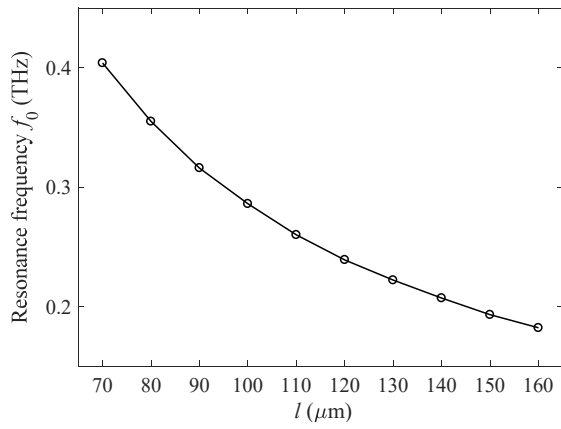


Figure 4: The resonance frequency as a function of  $l$ .

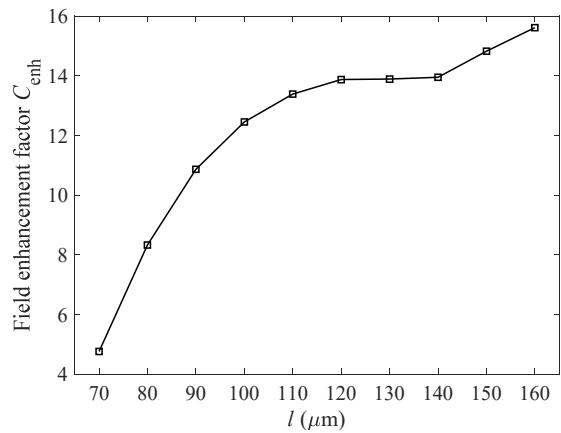


Figure 5: The field enhancement factor as a function of  $l$ .

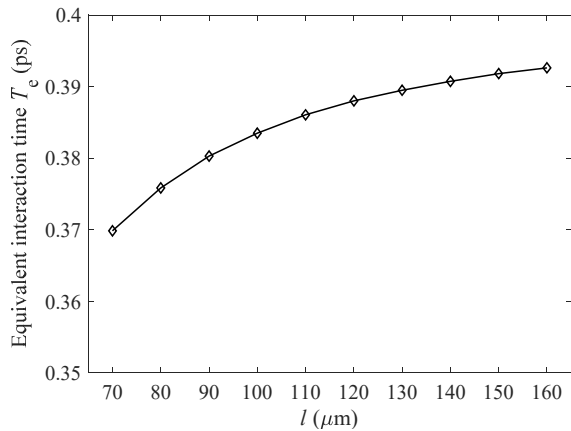


Figure 6: The equivalent interaction time as a function of  $l$ .

Figure 6 shows the  $l$  has little impact on the equivalent interaction time. This is expected since  $l$  only affects the resonance frequency and has no influence on the length of the interaction region. In Fig. 7, we show the production of all three parameters. As we can see, the highest  $F$  is obtained at  $l=100 \mu\text{m}$  which corresponds to the highest streak velocity and thus the smallest temporal resolution.

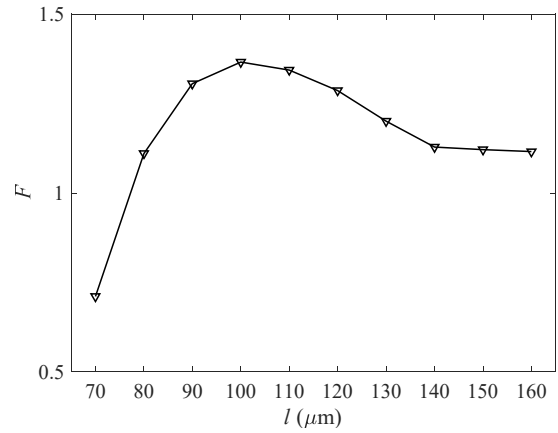


Figure 7: The parameter  $F$  as a function of  $l$ .

Next, we scan the parameter  $h$ . Other dimensions of the SRR are fixed at  $l=100 \mu\text{m}$ ,  $g=10 \mu\text{m}$ , and  $w=10 \mu\text{m}$ . In Fig. 8-10, we show the dependence of resonance frequency, field enhancement factor, and equivalent interaction time on  $h$ . As we can see, a larger  $h$  results in a longer the equivalent interaction time since it expands the interaction region. However, both the resonance frequency and field enhancement factor drop as we increase  $h$ . Such character of the square SRR indicates an optimal  $h$  may exists. The dependence of  $F$   $h$  is shown in Fig. 11. As we can see, the optimal  $h$  is about  $300 \mu\text{m}$  which increases the streak velocity about two times comparing to  $h=100 \mu\text{m}$ .

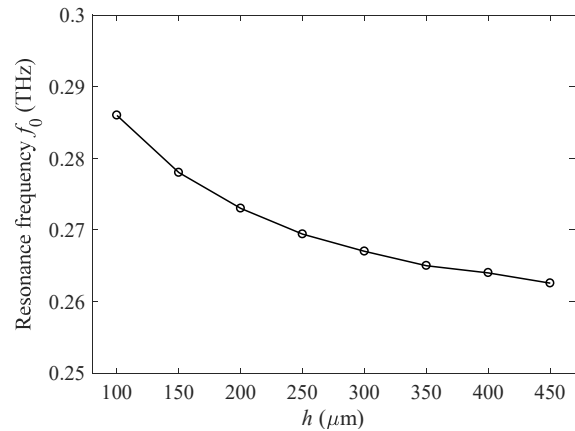


Figure 8: The resonance frequency as a function of  $h$ .

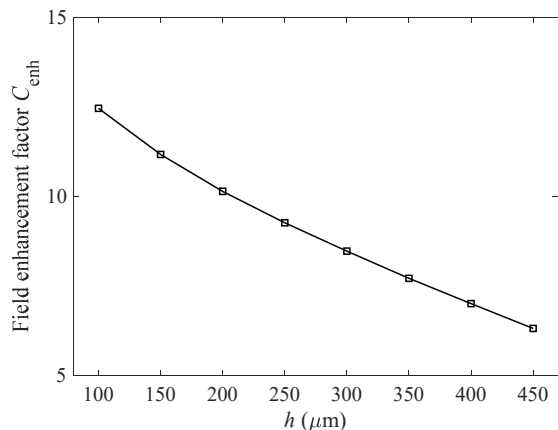


Figure 9: The field enhancement factor as a function of  $h$ .

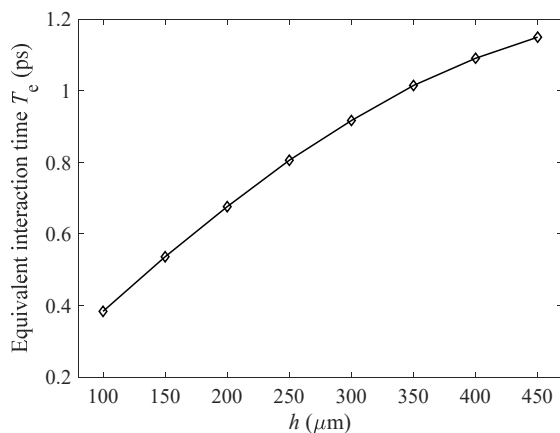


Figure 10: The equivalent interaction time as a function of  $h$ .

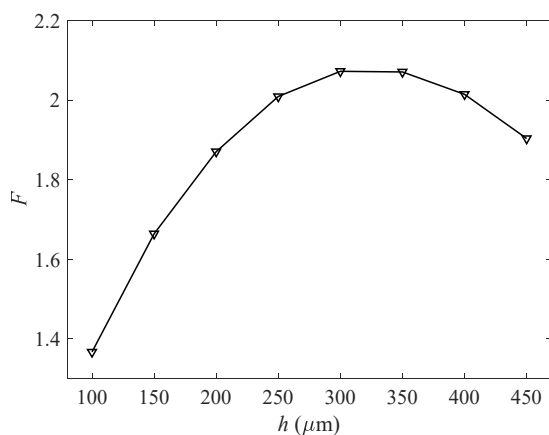


Figure 11: The parameter  $F$  as a function of  $h$ .

Eventually, we decide the final dimensions for the square SRR is  $l=100 \mu\text{m}$ ,  $h=100 \mu\text{m}$ ,  $g=10 \mu\text{m}$  and  $w=10 \mu\text{m}$ . Here we assume the peak streaking field is 50 MV/m and the unstreaked rms divergence is  $50 \mu\text{rad}$ , which are both practical according to recent experiment [10-12]. In this case, the temporal resolution calculated by Eq. (3) is about 6.15 fs. With improved efficiency in THz generation [13] and higher laser power, it is possible to increase the peak streak field to 500 MV/m level and reach a sub-fs temporal resolution.

## SUMMARY AND CONCLUSION

In this paper we study the dependence of streaking performance of a square SRR on its dimensions. By analytically deriving the expression for temporal resolution, we demonstrate that the temporal resolution of SRR is inversely proportional to three parameters which are the resonance frequency, field enhancement factor and the equivalent interaction time. The quantitative dependence of these three parameters on SRR dimensions is studied via CST simulation.

We focus on the  $l$  and  $h$  dimension of SRR. They decide the transverse and longitudinal size of the SRR. We find that SRR with larger  $l$  has a larger field enhancement factor

while the resonance frequency is smaller. This property indicates that an optimal  $l$  exists that produces the smallest temporal resolution. Meanwhile, if we increase  $h$ , the equivalent interaction time increases as well, but the resonance frequency and field enhancement factor both drop. Again, an optimal  $h$  is found to obtain the smallest temporal resolution. With the optimized dimension, the square SRR can provide sub-10 fs temporal resolution with 50 MV/m peak streak field.

Note that the optimization algorithm is preliminary which is used to reveal the dependence of streak performance on the SRR dimensions. A multi-dimensional single-objective optimization algorithm is required to realize a full and accurate optimization.

## REFERENCES

- [1] R. J. D. Miller, "Femtosecond crystallography with ultrabright electrons and x-rays: Capturing chemistry in action", *Science*, vol. 343, p. 1108-1116, 2014.
- [2] G. Sciani and R. Miller, "Femtosecond Electron Diffraction: Heraldng the Era of Atomically Resolved Dynamics", *Rep. Prog. Phys.*, vol. 74, p. 96101-96136, 2011.
- [3] I. Grgura *et al.*, "Ultrafast X-ray pulse characterization at free-electron lasers", *Nature Photonics*, vol. 6, p. 852-857, 2012.
- [4] J. Faure, *et al.*, "Controlled injection and acceleration of electrons in plasma wakefields by colliding laser pulses". *Nature* vol. 444, p. 737-739, 2006.
- [5] J. Maxson, *et al.*, "Direct Measurement of Sub-10 fs Relativistic Electron Beams with Ultralow Emittance". *Phys. Rev. Lett.*, vol. 118, p. 154802, 2017.
- [6] S. Park, *et al.*, "Measurement of low-energy and low-charge ultrashort bunches using an S-band RF deflector", *Nuclear instruments and methods in physics research*, vol. 927, p. 194-201, 2019.
- [7] J. Fabiańska, *et al.*, "Split ring resonator based THz-driven electron streak camera featuring femtosecond resolution", *Scientific Reports*, vol. 4, p. 5645, 2014.
- [8] H. Merbold, *et al.*, "Near field enhancement for THz switching and THz nonlinear spectroscopy applications", *CHIMIA International Journal for Chemistry*, vol. 65, p. 316-319, 2011.
- [9] C. Kealhofer, *et al.*, "All-optical control and metrology of electron pulses". *Science*, vol. 352, p. 429, 2016.
- [10] L. Zhao, *et al.*, "Terahertz streaking of few-femtosecond relativistic electron beams", *Physical Review X*, vol. 8, p. 021061, 2018.
- [11] R. Li, *et al.*, "Terahertz-based subfemtosecond metrology of relativistic electron beams", *Physical Review Accelerators and Beams*, vol. 22, 2019
- [12] X. L. Shen, *et al.*, "A THz driven split-ring resonator based ultrafast relativistic electron streak camera", *AIP advances*, vol. 9, p. 085209, 2019.
- [13] J. A. Fülöp, *et al.*, "Efficient generation of THz pulses with 0.4 mJ energy". *Optics Express*, vol. 22, p. 020155, 2014.